Pharm Res (2015) 32:2764–2774
DOI 10.1007/s11095-015-1662-x

RESEARCH PAPER

Nano-Targeted Delivery of Toremifene, an Estrogen Receptor-α Blocker in Prostate Cancer

Waseem Hariri • Thangirala Sudha • Dhruba J. Bharali • Huadong Cui • Shaker A. Mousa

Received: 16 October 2014 / Accepted: 2 March 2015 / Published online: 12 March 2015

ABSTRACT

Purpose Estrogen Receptor-α (ERα) expression is increased in prostate cancer and acts as an oncogene. We propose that blocking of estrogen hormone binding to ERα using the ERα blocker toremifene will reduce the tumorigenicity of prostate cancer, and nano-targeted delivery of toremifene will improve anticancer efficacy. We report the synthesis and use in an orthotopic mouse model of PLGA-PEG nanoparticles encapsulating toremifene and nanoparticles encapsulating toremifene that are also conjugated to anti-PSMA for targeted prostate tumor delivery.

Methods Human prostate cancer cell line PC3M and a nude mouse model were used to test efficacy of nano-targeted and nano-encapsulated toremifene *versus* free toremifene on the growth and differentiation of tumor cells.

Results Treatment with free toremifene resulted in a significant reduction in growth of prostate tumor and proliferation, and its nano-targeting resulted in greater reduction of prostate tumor growth, greater toremifene tumor uptake, and enhanced tumor necrosis. Tumors from animals treated with nano-encapsulated toremifene conjugated with anti-PSMA showed about a 15-fold increase of toremifene compared to free toremifene.

Conclusions Our data provide evidence that blocking ERα by toremifene and targeting prostate cancer tissues with anti-PSMA antibody on the nanoparticles' surface repressed the tumorigenicity of prostate cancer cells in this mouse model.

KEY WORDS anti-PSMA antibody · estrogen receptor-α blocker · nanomedicine · nano-targeted therapy · prostate cancer

Waseem Hariri and Thangirala Sudha contributed equally to this work.

W. Hariri • T. Sudha • D. J. Bharali • H. Cui • S. A. Mousa (✉)
The Pharmaceutical Research Institute, Albany College of Pharmacy and Health Sciences, 1 Discovery Drive, Rensselaer, New York 12144, USA
e-mail: shaker.mousa@acphs.edu

ABBREVIATIONS

ERα	Estrogen receptor alpha
ERβ	Estrogen receptor beta
HGPIN	High Grade Prostatic Intraepithelial Hyperplasia
MTT	3-(4, 5-dimethylthiazol-2-yl)-2, 5-diphenyltetrazolium bromide
PEG	Poly (ethylene glycol)
PLGA	Poly (lactic-co-glycolic acid)
PSMA	Prostate specific membrane antigen
SERM	Selective estrogen receptor modulator

INTRODUCTION

Prostate cancer is the most frequently diagnosed malignancy in American men. According to American Cancer Society statistics, in 2014 an estimated 233,000 new cases of prostate cancer will be diagnosed and about 29,480 patients are expected to die from it (1). It is also the second leading cause of cancer death in American males, exceeded only by lung cancer (2). The current treatment for prostate cancer depends on many factors like the patient's age, the stage (severity) of the cancer, and the patient's response to medical treatment including surgery and/or radiation (3,4), hormonal therapy (5,6), or chemotherapy (7–9). A tumor targeting approach is greatly needed to enhance anticancer efficacy and minimize adverse effects on normal organs. Despite tremendous effort by researchers in recent years to cure prostate cancer, it remains one of the most deadly diseases in the US. Therefore, it is imperative to look for alternative technologies that have the potential to overcome the inherent problems that are associated with current prostate cancer treatments.

Nanotechnology is an alternative technology that has had a profound impact in many medical fields including drug delivery and cancer detection, diagnosis, and treatment (10,11). Nanoparticles have special physical and chemical properties

that can be exploited for therapeutic purposes. Encapsulating chemotherapeutic drugs or other anticancer agents inside nanoparticles may result in less systemic toxicity compared to the free form of each drug. Surface tunable properties of the nanoparticles also enable conjugation of a cancer site-specific antibody or small molecule to increase the uptake of the nanoparticles and subsequently enhance drug efficacy (12).

For nano-targeting of prostate tumor, nanoparticles with a site-specific antibody Prostate Specific Membrane Antigen (PSMA), a highly specific prostate membrane antigen that is expressed on prostate cancer cells but minimally on normal cells, were synthesized and evaluated for efficacy in prostate cancer models. PSMA's expression on prostate cancer cells is 100 times more than on normal cells (13,14), and the site of expression is not typically exposed to circulating intact antibodies (15,16). In normal prostate tissue, PSMA exists primarily as a splice variant (PSM') that lacks the transmembrane domain (17,18), so when a cancer drug is conjugated with anti-PSMA antibody, it will be taken up only by the cancer cells that express the transmembrane domain of PSMA. In contrast to other prostate antigens like PSA and PAP that are secretory proteins, PSMA is an integral cell-membrane protein that is not secreted, which makes it an ideal target for monoclonal antibody therapy (19). Its level of expression increases as the cancer becomes more aggressive, which makes it a highly specific and sensitive marker to be used as a therapeutic target (20).

The small molecule toremifene is an FDA-approved selective estrogen receptor modulator (SERM) originally developed for treatment of metastatic breast cancer because it is a differentially selective ERα blocker. ERα is highly expressed in prostate cancer cells (21) and has a documented role as an oncogene in prostate cancer development, so blocking ERα by using a SERM like toremifene, which blocks only ERα, should stop the initial tumor formation. Toremifene has been evaluated in a multicenter, phase 2b dose-finding study in the treatment and prevention of High Grade Prostatic Intraepithelial Hyperplasia (HGPIN) using prostate cancer on follow-up biopsy as a primary end point. The conclusion was that toremifene decreased the incidence of prostate cancer by 1 year and had a tolerability profile comparable to that of placebo in a high-risk population (22). It is also believed that ERα plays an oncogenic role in prostate cancer and counteracts ERβ (23). However, the major problem associated with toremifene, like many other anticancer agents, is its solubility (it is soluble in organic solvent) and adverse side effects. The use of nanoparticles may overcome these major problems *via* an injectable formulation that would have minimum side effects. Furthermore, the advantages of using nanotechnology might minimize the toxicity of chemotherapeutic agents, protect the drugs from inactivation by metabolic enzymes, reduce renal clearance, and decrease drug resistance by targeting cancer cells.

In the current study we encapsulated toremifene in nanoparticles and conjugated the nanoparticles with anti-PSMA for targeted delivery of toremifene to prostate tumor in an orthotopic mouse model and compared its bioavailability in tumor with free toremifene and with nanoformulations of toremifene. This investigation represents the first report on the nano-formulation of toremifene for targeted delivery into prostate tumor.

MATERIALS AND METHODS

Cancer Cell Lines and Reagents

PC3M cancer cells were obtained from Dr. T. Arumugam (MD Anderson Cancer Center, Houston, TX, USA). Cell culture medium, Dulbecco's Modified Eagle Medium (DMEM), fetal bovine serum (FBS), penicillin, streptomycin, toremifene base, and other common reagents were purchased from Sigma-Aldrich (St Louis, MO, USA). Cell growth determination kit (MTT kit) was purchased from Life Technologies (Grand Island, NY, USA). Antibodies for the flow cytometry (ERα and PSMA antibodies) were purchased from Abcam (Cambridge, MA, USA). Poly (lactic acid-co-glycolic acid)—poly (ethylene glycol) (PLGA-PEG) and maleimide-PLGA-PEG were purchased from Polyscitech (West Lafayette, IN, USA).

Nanoparticle Synthesis

For the preparation of PLGA-PEG nanoparticles encapsulating toremifene, 1 ml PLGA-PEG and maleimide-PLGA-PEG in a ratio of 9:1 (80 mg/ml) were mixed with 200 μl of toremifene (20 mg/ml DMSO). This solution was added to 100 ml of 1% polyvinyl alcohol solution drop-by-drop under constant magnetic stirring. It was then sonicated in a probe sonicator for 30 s and stirred for another 12 h. Finally, the solution was dialyzed for 48 h using a filter with molecular weight cutoff 500–1000, changing the deionized water outside the bag 4 times every 12 h to remove impurities and residual DMSO (24). Conjugation of anti-PSMA to the PLGA-PEG nanoparticles encapsulating toremifene was done by first thiolating the anti-PSMA antibody using Traut's reagent (25,26). The thiolated anti-PSMA can readily react with the maleimide group (25).

Nanoparticle Size Distribution

The size distribution of nanoparticles synthesized in this study (void PLGA-PEG nanoparticles, PLGA-PEG nanoparticles encapsulating toremifene, and PLGA-PEG nanoparticles encapsulating toremifene and conjugated to anti-PSMA) in aqueous dispersions were determined with dynamic laser light

scattering (DLS) using a Malvern zeta sizer (Malvern Instrumentation Co, Malvern, PA USA). For each nanoparticle solution, one ml was transferred into a 3 ml, 4-sided clear plastic cuvette and measured directly.

Nanoparticle Size and Morphology

The size and morphology of PLGA-PEG nanoparticles encapsulating toremifene and PLGA-PEG nanoparticles encapsulating toremifene and conjugated to anti-PSMA were examined by transmission electron microscopy (TEM) using a JEOL JEM-100CX transmission electron microscope (JEOL USA, Inc., Peabody, MA). One drop of the nanoparticles solution was mounted on a thin film of amorphous carbon deposited on a copper grid (300 mesh). The solution was air dried, and the sample was examined directly under the microscope.

Entrapment Efficiency (Loading Efficiency)

The amount of toremifene encapsulated in the nanoparticles was determined by disintegrating the nanoparticles and measuring the toremifene in duplicate with HPLC. This also helps in determination of the entrapment efficiency of toremifene in the nanoformulation. The nanoparticles were disintegrated by adding a 10-fold volume of 100% acetonitrile and then sonicating for 3 min, then diluting 10-fold with 70% acetonitrile. After centrifugation at 15,000×*g* for 5 min, the resulting solution was analyzed using a modified HPLC method (27,28) with a Sunfire C18 column, 3.0×50 mm, 3.5 μm (Waters, Milford, MA, USA), and a UV detector at 254 nm. The mobile phase consisted of 75% acetonitrile containing 0.1% formic acid, and the flow rate was 0.35 ml/min. The entrapment efficiency was determined with the formula in Eq. 1:

$$entrapment\ \ efficiency(loading) = \left([toremifene]_f\right)/\left([toremifene]_t\right) \times 100 \quad (1)$$

where $[\text{toremifene}]_f$ is the concentration of toremifene in the centrifugate and $[\text{toremifene}]_t$ is the theoretical concentration of toremifene (meaning total amount of toremifene added initially). The amount of nano-encapsulated toremifene used in all *in vitro* and *in vivo* experiments in this study was determined using this established HPLC method.

Cell Culture

Human prostate cancer cells PC3M were cultured in DMEM containing 10% FBS, 1% penicillin, and 1% streptomycin. Cultures were maintained in a 37°C humidified chamber with 5% CO_2. Media was changed every 3 days, and the cell lines were passaged at 80% confluence.

Flow Cytometry

To analyze the expression of ERα and PSMA in the PC3M cells, cells were cultured to sub-confluence and treated with 0.25% (w/v) trypsin/EDTA to release from culture flask. Cells were fixed in 1% paraformaldehyde and then permeabilized with 0.05% triton-X100. After washing with PBS, the cells were incubated with anti-ERα or anti-PSMA at 4°C overnight. To detect the proteins, cells were incubated with secondary antibody conjugated with fluorescein isothiocyanate (FITC) or phycoerythrin (PE) in the dark for 30 min and analyzed with flow cytometry (BD Biosciences, San Jose, CA, USA).

MTT Assay

PC3M cells were subjected to treatment with toremifene at concentrations ranging from 1.0 to 100 μM. After 24, 48, and 72 h of exposure to the drug, cell viability was determined by the MTT viability assay (3-(4,5-dimethylthiazol-2-yl)-2,5-diphenyltetrazolium bromide), as per the manufacturer's protocol. Briefly, cells were seeded at a density of 10^4 cells/well in 96-well plates, and then incubated with toremifene. After treatment, 100 μl from 5 mg/ml of MTT solution in PBS at pH 7.4 was added to each well, and plates were incubated for 4 h at 37°C. The MTT formazan formed in the different wells was solubilized by the addition of 50 μl of DMSO and incubated for 10 min at 37°C (29). The optical density of each well was determined using an ELISA plate reader at an activation wavelength of 570 nm and reference wavelength of 650 nm. The percentage of viable cells was determined by comparison to untreated control cells where the optical density correlates with the percentage of cell viability.

Animal Studies

The animal studies were performed in accordance with institutional guidelines for animal safety and welfare at the animal facility of the Albany Stratton Veterans Affairs Medical Center (Albany, NY, USA), and the experimental protocol was approved by the Institutional Animal Care and Use Committee of the Veterans Affairs Medical Center. Athymic nude male mice of 6–8 weeks of age and weighing approximately 20 g were purchased from Harlan Laboratories, Inc. (Indianapolis, IN, USA). They were allowed to acclimate for 5 days prior to the initiation of treatment. The animals were housed under standard conditions (in laminar airflow cabinets under pathogen-free conditions with 12 h light/12 h dark schedule) and fed with autoclaved water and Harlan Teklad sterilizable diet.

PC3M cells were implanted by surgical orthotopic implantation in the lateral lobe of the prostate in each animal. The animals were kept under isoflurane anesthesia during surgery.

A lower midline abdominal incision was made. After proper exposure of the bladder and prostate, 0.25×10^6 cells/20 μl medium were implanted into the prostate based on the established calibration curve for the number of cells *versus* optical density. The incision in the abdominal wall was closed with clips, and the animals were monitored until they recovered. Two days after tumor implantation, 7–8 mice were randomly assigned into each of 5 groups. For 3 weeks mice received daily subcutaneous injection of either PBS (control), void nanoparticles, toremifene citrate (1.5 mg/kg body weight), nano-encapsulated toremifene (1.5 mg/kg body weight), or nano-encapsulated toremifene (1.5 mg/kg body weight) conjugated with anti-PSMA where all were dispersed in PBS, pH 7.4. Body weights were measured twice a week. Twenty-four h after the last treatment, all mice were sacrificed and tumors, livers, and kidneys were harvested. Tumor weight was measured, and blood samples were collected from each animal. Levels of toremifene in all the samples were measured as described in the biodistribution study below.

Histopathology

Half of the tumor tissues were fixed in phosphate-buffered formalin and embedded in paraffin. Paraffin blocks were cut by microtome to prepare slides, and the sections were stained with hematoxylin and eosin (H&E). Ten images from each tumor were analyzed and the percentage of necrotic areas in the tumor tissue sections was estimated under the microscope. The analysis was carried out by two investigators independently, and the results were compared.

Biodistribution Study

Toremifene concentration in mouse plasma was measured with HPLC and in tissue homogenates with liquid chromatography tandem mass spectrometry (LC-MS/MS) using an API 4000 triple-quadrapole mass spectrometer (Applied Biosystem MDS Sciex, Toronto, Canada) using a modification of reported methods for toremifene (27,28). Briefly, plasma (0.1 ml) or tissue homogenate (0.25 g/ml) was extracted using 1.25 ml of a mixture of hexane/n-butanol (98:2, v/v). Samples were vortexed for 10 min and centrifuged at 22, 000×*g* for 10 min. The solvent phase was transferred to a clean test tube and evaporated with nitrogen. The residue was resuspended in 0.15 ml 70% acetonitrile containing 0.1% formic acid. The resulting sample was separated using an Oasis HLB column, 4.6×20 mm, 25 μm (Waters) with a gradient elution of 0.85 ml/min for 10 min. The mobile phase was A: 0.1% formic acid, B: acetonitrile containing 1.0% formic acid, and the gradient program was (time in min/%B): 0–1.5/30%, 1.6–4/95%, and 4.1/30%. The injection volume was 20 μl. The tandem mass spectrometer was operated in positive electrospray mode with the ion spray voltage set at 3.5 KV and temperature set at 450°C. Toremifene was detected using multiple reaction monitoring, and quantitation was achieved by monitoring mass transition 406.2/252.1 (m/z). All data were acquired and processed with Analyst 1.4.2 software (Applied Biosystem MDS Sciex). The limit of detection was 15 pg, and the limit of quantitation was 1.65 ng/ml.

Statistical Analysis

Statistical analysis was performed using StatCrunch™ software and Excel. One-way ANOVA was used to compare the mean±SEM from each experimental group with its respective control group. Statistical differences approaching $P<0.05$ were considered statistically significant.

RESULTS

Expression of Prostate Cancer Proteins and ERα in PC3M (Variant)

Flow cytometry analysis showed that more than 95% of PC3M cells were positive for both ERα proteins (Fig. 1a1 and a2) and PSMA (Fig. 1b1 and b2). In contrast, parent PC3 showed lack of PSMA expression as compared to the high expression level in the PC3M (data not shown).

Effect of Toremifene on Prostate Cancer Cell Viability

The effect of toremifene on prostate cancer cell viability was determined by subjecting PC3M cells to treatment with increasing concentrations of toremifene for 24, 48, and 72 h (Fig. 2a–c). Toremifene inhibited cellular proliferation in a concentration-dependent manner, with a maximum effect at 20 μM. There was a significant reduction on the cells' viability by 50% after treating cells with 10–20 μM of toremifene in the first 24 h (Fig. 2a). With an increase in the duration of exposure to toremifene, viability of PC3M cells decreased as seen at 48 h and 72 h (Fig. 2c). The decrease of cancer cell viability ranged from ~50% (at 24 h) to ~65% (at 48 h) and ~70% (at 72 h) with 20 μM toremifene (Fig. 2).

Nanoparticle Size Distribution and Morphology

The average size of the PLGA-PEG nanoparticles encapsulating toremifene was 252 nm and of the PLGA-PEG nanoparticles encapsulating toremifene and conjugated to anti-PSMA was 248 nm as measured with the zeta size analyzer (Fig. 3a and b). The nanoparticle size observed with TEM was comparable to that observed with DLS, and the nanoparticles were spherical (Fig. 3c and d).

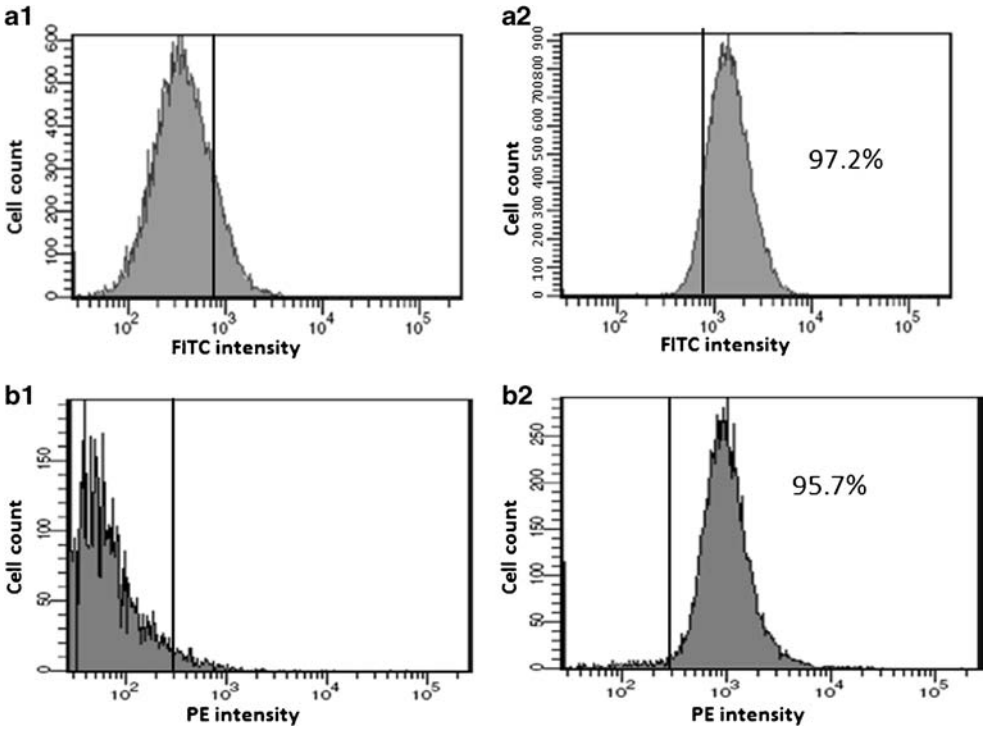

Fig. 1 Flow cytometry analysis of PC3M (variant) cell line and its expression ability of (**a1**) unstained PC3M cells under FITC profile, (**a2**) PC3M cells incubated with anti-estrogen receptor α (ERα) and detected with FITC secondary antibody showing 97.2% are positive for ER α, (**b1**) unstained PC3M cells under PE profile, and (**b2**) PC3M cells incubated with anti-Prostate Specific Membrane Antigen (PSMA) and detected with PE conjugated secondary antibody showing 95.7% are positive for PSMA. In contrast, PC3 prostate cancer cell lines did not express PSMA (not shown). Abbreviations: *FITC* fluorescein isothiocyanate; *PE* phycoerythrin.

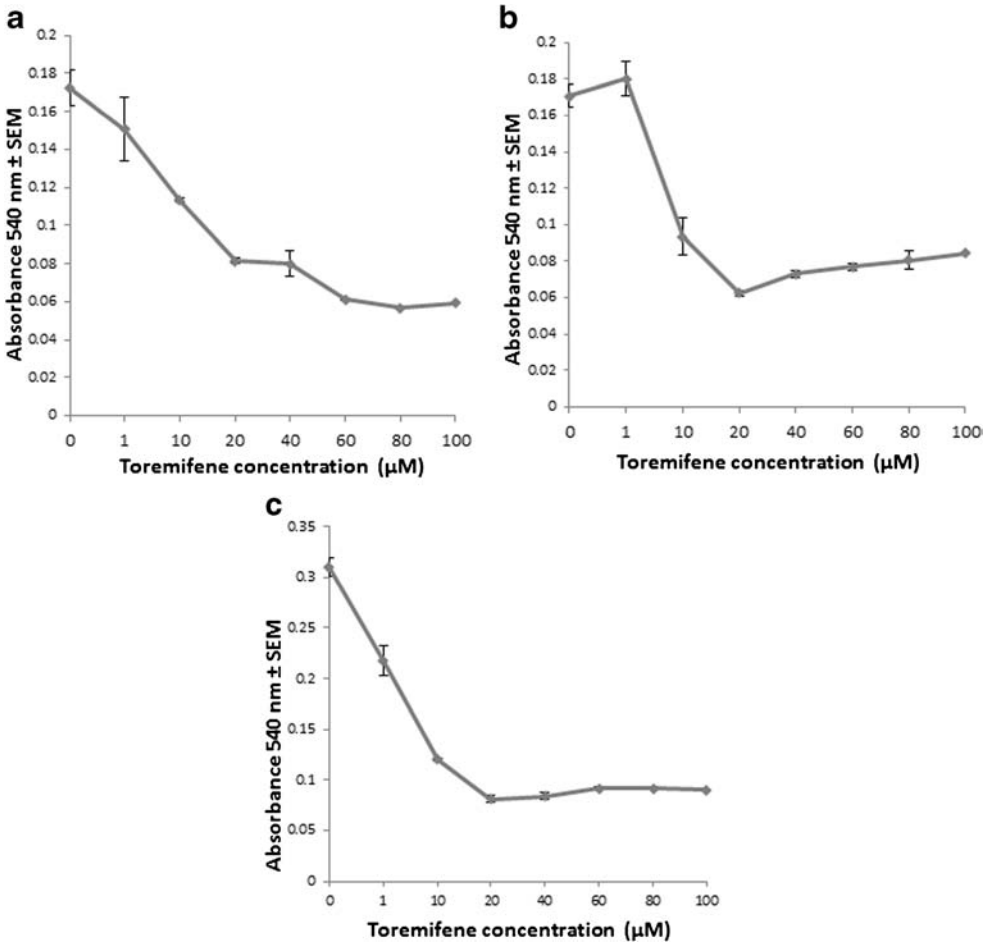

Fig. 2 The effects of free toremifene on PC3M cells' viability using different toremifene concentrations (μM/well) and measured with the MTT assay after incubation at 37°C for (**a**) 24 h, (**b**) 48 h, and (**c**) 72 h. Data represent mean ± SEM, $n = 3$.

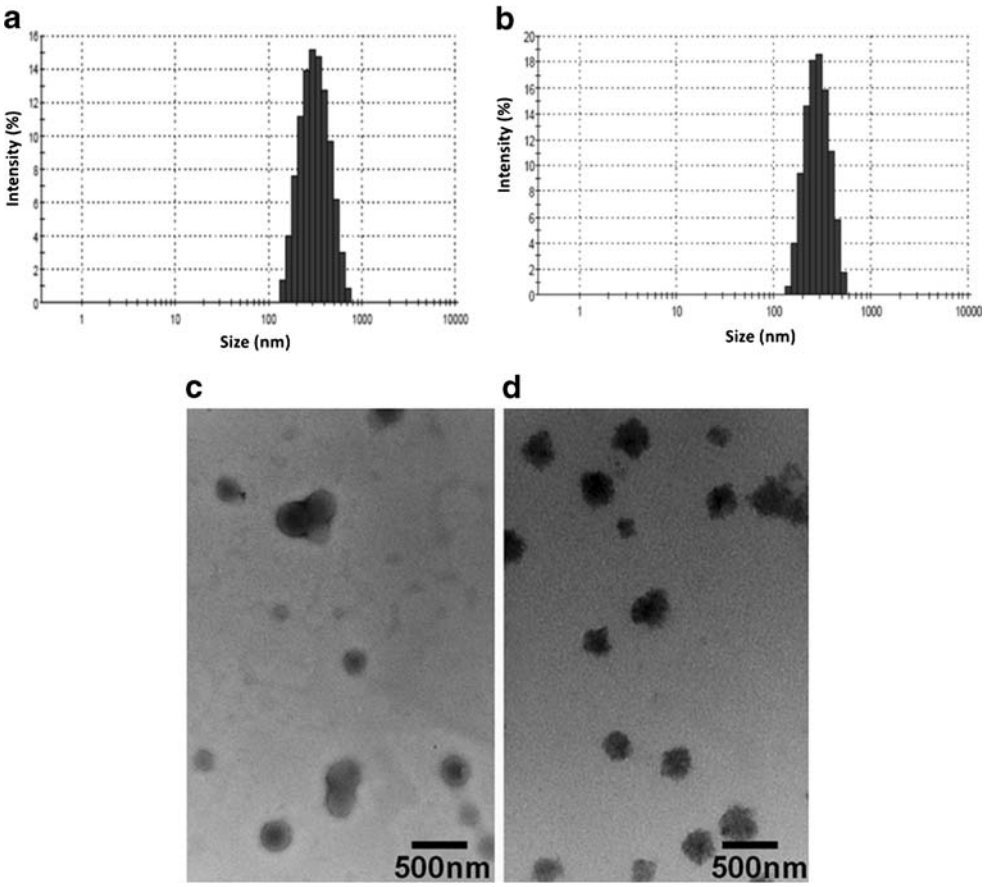

Fig. 3 Nanoparticle size distribution determination with dynamic light scattering and nanoparticle size and morphology examination by transmission electron microscopy of (**a**, **c**) PLGA-PEG nanoparticles encapsulating toremifene (Z average size = 252 nm in diameter), (**b**, **d**) PLGA-PEG nanoparticles encapsulating toremifene and conjugated with anti-PSMA antibody (Z average size = 248 nm in diameter).

Anti-Tumorigenic Effect of Toremifene in *In Vivo* Studies

We observed that when animals were treated with higher doses of toremifene (>1.5 mg/kg body weight), toremifene accumulated in high concentrations in the liver and kidneys (data not shown). At the end of the current study, tumor weights were measured and compared with the control groups treated with PBS. The average weight of the excised tumors was significantly decreased in mice treated with toremifene compared to animals treated with PBS alone (positive control), $P=0.0034$.

Comparison of Tumor Growth Suppression by Toremifene and Its Nanoformulations

To study the effect of nano-encapsulated toremifene and its PSMA conjugated nanoformulation on the orthotopic prostate tumor, animals were treated for 3 weeks with PBS (control), void nanoparticles, toremifene, nano-encapsulated toremifene, or nano-encapsulated toremifene conjugated with anti-PSMA. Tumor weights showed statistically significant reductions between toremifene and nano-encapsulated toremifene and nano-encapsulated toremifene conjugated with anti-PSMA antibody ($P<0.0001$) (Fig. 4). There was a statistically significant difference in the tumor weight between animals treated with free toremifene and nano-encapsulated toremifene conjugated with anti-PSMA antibody ($P=0.0033$) (Fig. 4). There was no significant tumor weight reduction between the positive control and the void nanoparticles (Fig. 4).

Biodistribution of Toremifene in Tumor and Other Organs After Treatment

To compare the levels of toremifene in the tumors as a result of the various treatments, toremifene levels were measured in tumors at the end of the study. The concentration of toremifene was also measured in blood, liver, and kidney and compared with free toremifene and nano-encapsulated toremifene without targeting. In tumors from animals treated with nano-encapsulated toremifene conjugated with anti-PSMA there was about a 15-fold increase of toremifene compared to free toremifene (Fig. 5a and Table I). Serum from the animals treated with nano-encapsulated toremifene with anti-PSMA antibody showed a 9-fold increase of toremifene compared with free toremifene (Fig. 5b and Table I). In the liver and kidney, there was only a 4-fold increase of toremifene in the nano-encapsulated toremifene conjugated anti-PSMA treatment group compared to treatment with free toremifene

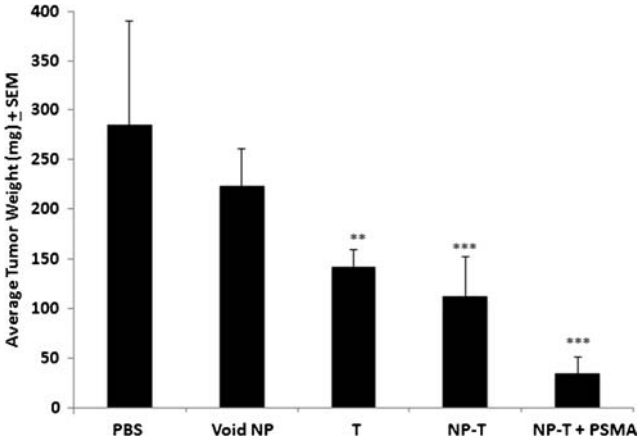

Fig. 4 Nano-encapsulated toremifene conjugated with anti-PSMA reduced prostate tumor weight significantly compared to other groups in nude mice orthotopically implanted with prostate (PC3M) cancer cells. Data represent mean tumor weight ± SEM. The number of animals per group ranged from 7 to 8. ** $P < 0.01$, *** $P < 0.0001$. Abbreviations: *NP* nanoparticles; *T* toremifene; *NP-T* nano-encapsulated toremifene; *NP-T + PSMA* nano-encapsulated toremifene conjugated with anti-PSMA.

(Fig. 5c, d and Table I). In the animals treated with nano-encapsulated toremifene, tumor and serum had a 3- to 4-fold increase, and liver and kidney showed a nominal increase compared with free toremifene treatment (Fig. 5 and Table I).

Comparing targeted *versus* non-targeted nano-encapsulated toremifene, there were statistically significant 5- to 6-fold increases in toremifene tumor levels and 2- to 3-fold increases in toremifene levels in serum, but no statistically significant differences in either kidney or liver uptake (Table I). Hence, nano-encapsulated toremifene conjugated with anti-PSMA exhibited a remarkable increase in toremifene levels by about 15-fold as compared to free toremifene (Fig. 5a).

Effect of Toremifene on Tumor Cell Necrosis

To study the viability of the tumors, an indication of the manifestation of disease, H&E stained sections of the tumors were analyzed. The control group showed aggressive growth of the tumor cells, with a high number of mitotic figures and few necrotic areas (Fig. 6b1, b2, and b3). After treatment with either nano-encapsulated toremifene or nano-encapsulated toremifene conjugated with anti-PSMA, tumors showed significant reduction in the survival rate of tumor cells and few mitotic figures along with large necrotic areas (Fig. 6c1, c2). Control group, void nanoparticles, and free toremifene treated groups showed highly proliferating cells with few necrotic cells compared to nanoformulations (Figs. 6 and 7). There were no significant differences between nano-encapsulated toremifene and nano-encapsulated toremifene conjugated with anti-PSMA antibody in terms of the necrotic area and the mitotic figures (Fig. 7).

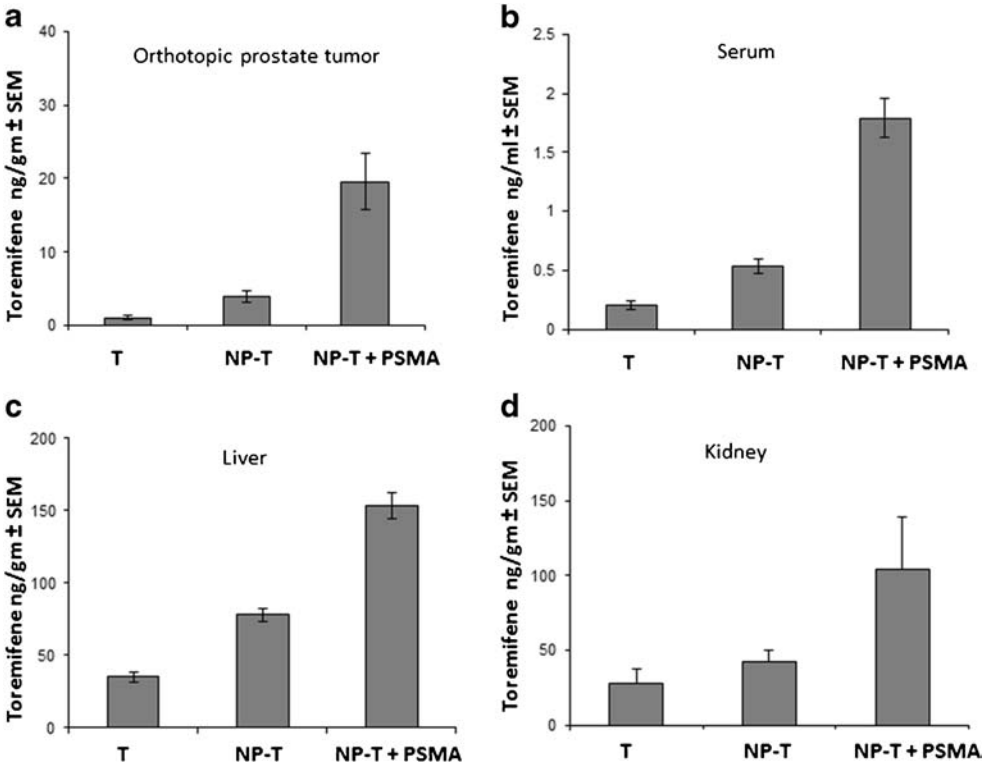

Fig. 5 Biodistribution of toremifene in tumor, serum, liver, and kidney after treatment with free toremifene (*T*), nano-encapsulated toremifene (*NP-T*), and nano-encapsulated toremifene conjugated with anti-PSMA (*NP-T + PSMA*). Data represent mean ± SEM, $n = 7$–8 mice per group. (**a**) Tumor levels of toremifene. There is about a 15-fold increase in the NP-T + PSMA group compared to free toremifene. (**b**) Serum levels of toremifene. There is a 9-fold increase in toremifene concentration in the NP-T + PSMA group compared to the free toremifene group. (**c**) Liver homogenate levels of toremifene. (**d**) Kidney homogenate levels of toremifene.

Table I Biodistribution of Toremifene (−Folds Compared to Free Toremifene) in Prostate Tumor and Serum, Kidney, and Liver After Treatment With Non-Targeted Nano-Encapsulated Toremifene *Versus* Targeted Nano-Encapsulated Toremifene Conjugated with Anti-PSMA

Group	Toremifene level (−folds)			
	Tumor	Serum	Kidney	Liver
Nano-encapsulated toremifene	3.73 ± 0.67	2.7 ± 0.3	1.51 ± 0.11	2.23 ± 0.13
Nano-encapsulated toremifene conjugated with anti-PSMA	14.87 ± 3.31**	8.96 ± 0.8*	3.73 ± 0.45	4.37 ± 0.24

Data represent mean (−fold changes of toremifene levels compared to free toremifene) ± SEM, $n = 7–8$ animals per group. *$P < 0.05$, **$P < 0.01$

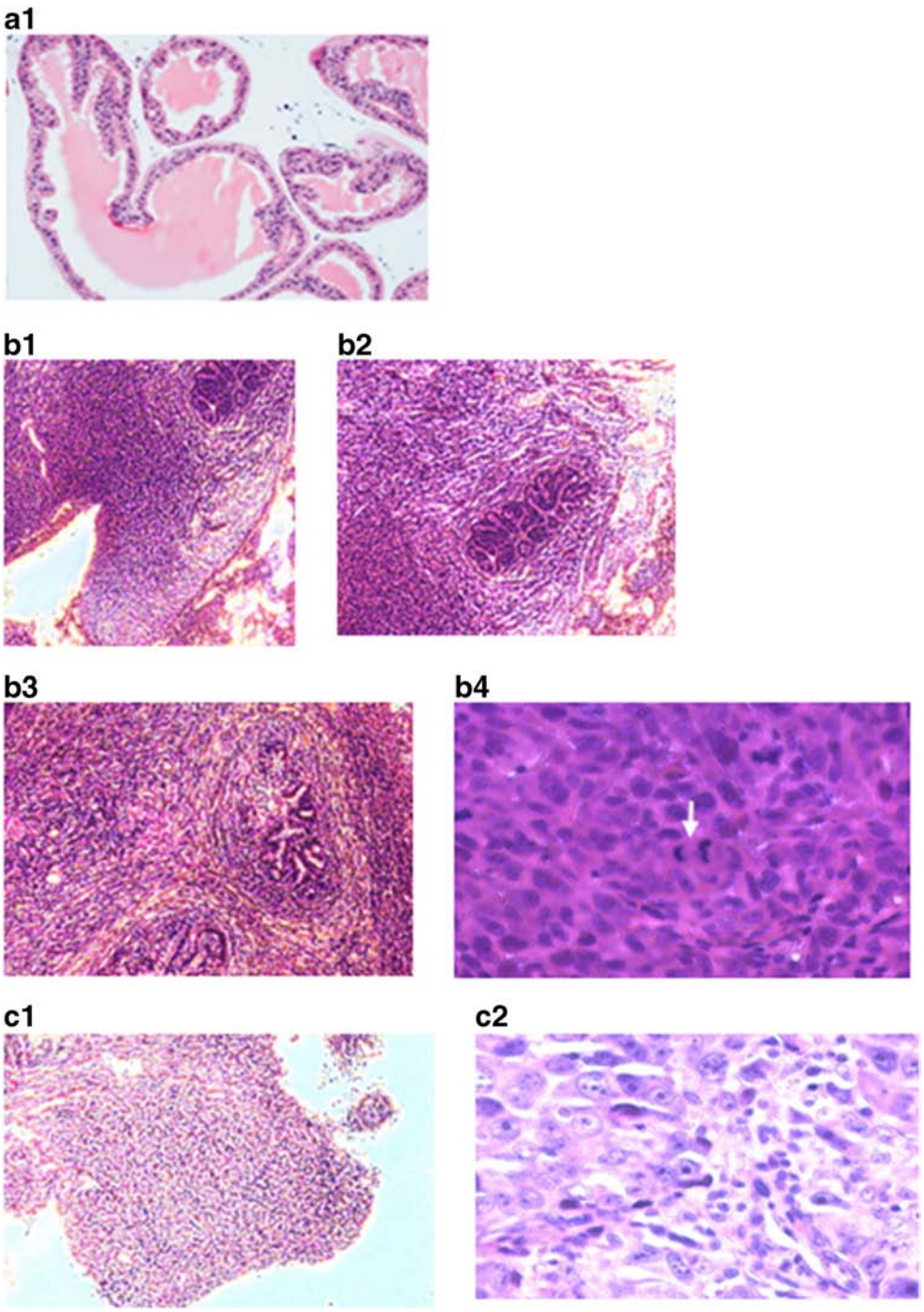

Fig. 6 Representative H&E histological staining of normal prostate *versus* prostate tumor in nude mice treated with toremifene, nano-encapsulated toremifene, and nano-encapsulated toremifene conjugated with anti-PSMA. Normal prostatic tissue (**a**) illustrating a well-defined gland with single layer epithelium, and clear cytoplasm (Mag. 5×). Control group (**b1**–**b4**). **b1** shows cancer cells overgrowth with small necrotic area (Mag. 5×). **b2** shows an invasion of the cancer cells to a gland without destroying its structure (Mag. 5×). **b3** shows a total infiltration and destruction of most of the gland by the cancer cells (Mag. 5×). **b4** shows an active mitotic figure (*arrow* points to anaphase stage) (Mag. 20×). (**c1**–**c2**) **c1** shows a large area of necrotic cells due to treatment with nano-encapsulated toremifene conjugated with anti-PSMA (Mag. 5×). **c2** shows a large number of cells with condensed chromatin and shrunken nucleoli (Mag. 20×). A few cells have already fragmented and lost their membrane integrity.

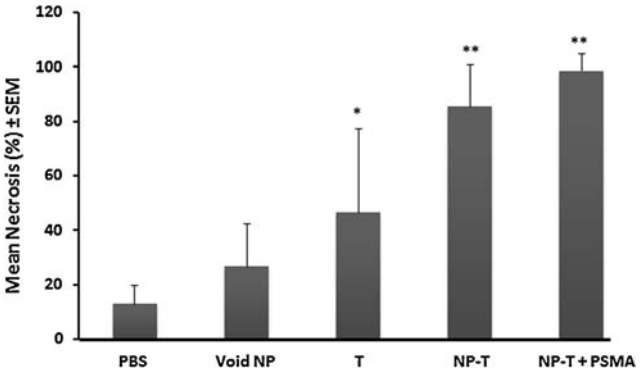

Fig. 7 Nano-encapsulated toremifene conjugated with anti-PSMA significantly increased the percentage of necrosis in the tumor tissues of the male nude mice compared to other groups: *PBS* (control), void nanoparticles (*NP*), free toremifene (*T*), nano-encapsulated toremifene (*NP-T*), or nano-encapsulated toremifene conjugated with anti-PSMA (*NP-T + PSMA*). H&E stained sections were analyzed by two independent investigators for necrosis and tumor areas. The error bars show ± SEM of each group. * $P = 0.0066$, ** $P < 0.0001$.

DISCUSSION

The present study shows that the efficacy of toremifene when encapsulated in PLGA-PEG nanoparticles increased by 4-fold compared to free toremifene in suppressing the prostate cancer tumor in this mouse model. Nano-encapsulated toremifene conjugated with anti-PSMA antibody exhibited a remarkable increase in toremifene levels (by several folds) in the prostate tumor cells, confirming the targeted delivery capacity of this toremifene nanoformulation. This supports our hypothesis that site-directed delivery of a nanoformulation (by conjugating tumor-targeting ligands) encapsulating a chemotherapeutic drug (toremifene) can enhance the efficacy of the drug by many folds due to the enhanced accumulation of the drug in the cancer site (10,30). We successfully encapsulated toremifene in nanoparticles and also conjugated them with anti-PSMA and developed a method to quantitate the loading level in the nanoformulation with HPLC and LC-MS/MS.

Expression of ERα and ERβ has been reported to be differently expressed in human prostate cancer cell lines, including the androgen sensitive LNCaP (ERα−/ ERβ +) and the androgen-insensitive PC-3 (ERα +/ ERβ +) and PC3M (ERα +/ ERβ +) (21,31). Here, at lower concentrations (10–20 μM), toremifene reduced PC3M cells' viability and proliferation. This strong inhibition with a low dose of toremifene could be explained by the higher level of expression of ERα on the stromal surface of the PC3M cancer cells. This supports the idea that ERα is playing a role in transcriptional stimulation and cellular proliferation of the prostate cancer (23).

The use of orthotopic models of human prostate cancer in the nude mouse replicates human disease with high fidelity and allows for testing of novel treatment strategies as shown here. Compared to the positive control (PBS group), mice treated with free toremifene showed a statistically significant decrease of tumor growth (tumor weight) of orthotopically implanted PC3M cells, reflecting the significant effect of free toremifene in treating prostate cancer compared to a non-treated group as reported by Raghow *et al.* in a prostate cancer transgenic mice model (11). This effect could show the significant blockage of ERα and its important role in developing and maintaining the growth of prostate cancer.

As per as our hypothesis, the nanoparticles encapsulating toremifene and conjugated to anti-PSMA antibody were the most significant treatment and inhibited the tumor growth. The statistically significant growth inhibition between nano-encapsulated toremifene and nano-encapsulated toremifene conjugated with anti-PSMA antibody could mean that PSMA is not only a diagnostic marker but a therapeutic target as well. The biodistribution studies showed that nano-encapsulated toremifene conjugated with anti-PSMA antibody had the highest concentration of the chemotherapeutic drug (about 15-fold) in the tumor tissue when compared to the free toremifene or nano-encapsulated toremifene without conjugation (4-fold compared to free toremifene); these results indicate that conjugation with anti-PSMA did target the nanoparticles toward the prostate tumor effectively. Our null hypothesis was accepted because both nano-encapsulated toremifene and nano-encapsulated toremifene conjugated with anti-PSMA antibody exhibited remarkably significant inhibition of tumor growth that is correlated to the level of toremifene delivered into the prostate tumor.

Histopathological studies showed that most of the excised tumor masses from mice treated with nano-encapsulated toremifene were necrotic, which showed the efficacy of the nano-encapsulation of toremifene compared to its free form.

The data showed that nano-encapsulated toremifene conjugated with anti-PSMA antibody was better in terms of targeting the therapy than both the free toremifene and nano-encapsulated toremifene without anti-PSMA antibody. In plasma, a high detectable level (9-fold more than free toremifene) of toremifene in the anti-PSMA nano-encapsulated toremifene-treated animals was an indication of the high bioavailability of the toremifene in the circulation. The slightly high levels of toremifene (4-fold more than free toremifene) of nano-encapsulated toremifene conjugated with anti-PSMA antibody observed in liver and kidney could be due to high metabolism of toremifene by the liver, the expression of PSMA in renal tubule (32), the long half-life of PLGA-PEG nanoparticles, or the continuous release of toremifene from PLGA-PEG. Issues with hepatotoxicity and nephrotoxicity may be possible and therefore reducing the dose of nano-encapsulated toremifene conjugated with anti-PSMA antibody might be an alternative for optimal efficacy and safety.

Nano-encapsulated toremifene shows higher efficacy than free toremifene in suppressing prostate cancer tumor growth both *in vitro* and *in vivo*. Nano-encapsulated toremifene shows

even higher efficacy when conjugated to a targeted moiety like anti-PSMA specific to prostate cancer tumor. The encapsulation of toremifene inside the nanoparticles provided more efficient and targeted delivery to the prostate cancer tumor than free toremifene. Our data provide evidence that blocking ERα by toremifene and targeting the prostate cancer tissues specifically by conjugating anti-PSMA antibody on the surface of the nanoparticles repressed the tumorigenicity of prostate cancer cells in this mouse model. Furthermore, targeted delivery of nanoconjugated (nano-targeted) toremifene caused remarkably greater necrosis of the prostate cancer cells compared with free toremifene. It follows that nano-targeted delivery approaches have potential to enhance the delivery of toremifene to multiple targets of prostate cancer and improve its efficacy. Additionally, nano-targeting is expected to provide tumor-guided imaging for personalized monitoring of the optimal duration of therapy that leads to maximal eradication of the tumor.

CONCLUSION

Toremifene significantly reduces growth of PC3M cells *in vitro* and *in vivo*, and prostate cancer nano-targeted toremifene increased its anticancer efficacy and caused greater necrosis of the cancer cells as compared to free toremifene in this orthotopic mouse model.

ACKNOWLEDGMENTS AND DISCLOSURES

We would like to express our thanks to Dr. Murat Yalcin (Uludag University, Turkey) and Dr. Hasan Mukhtar (University of Wisconsin, Madison, WI) for their suggestions, and Dr. Kelly Keating (ACPHS) for excellent editing. The authors report no conflicts of interest.

REFERENCES

1. American Cancer Society. Cancer Facts & Figures 2014. 2014 September 10. Available from: http://www.cancer.org/acs/groups/content/@research/documents/webcontent/acspc-042151.pdf.
2. Siegel R, Naishadham D, Jemal A. Cancer statistics, 2012. CA Cancer J Clin. 2012;62(1):10–29.
3. Khadige M, Peiffert D, Supiot S. What is the level of evidence of new techniques in prostate cancer radiotherapy? Cancer Radiother. 2014;18(5–6):501–8.
4. Fizazi K, Scher HI, Miller K, Basch E, Sternberg CN, Cella D, *et al.* Effect of enzalutamide on time to first skeletal-related event, pain, and quality of life in men with castration-resistant prostate cancer: results from the randomised, phase 3 AFFIRM trial. Lancet Oncol. 2014;15(10):1147–56.
5. Stewart SB, Cheville JC, Sebo TJ, Frank I, Boorjian SA, Thompson RH, *et al.* Gleason grading after neoadjuvant hormonal therapy retains prognostic value for systemic progression following radical prostatectomy. Prostate Cancer Prostatic Dis. 2014;17(4):332–7.
6. Ziehr DR, Chen MH, Zhang D, Braccioforte MH, Moran BJ, Mahal BA, *et al.* Association of androgen deprivation therapy with excess cardiac-specific mortality in men with prostate cancer. BJU Int. 2014. doi:10.1111/bju.12905.
7. Lee HY, Wu WJ, Huang CH, Chou YH, Huang CN, Lee YC, *et al.* Clinical predictor of survival following docetaxel-based chemotherapy. Oncol Lett. 2014;8(4):1788–92.
8. Gordon RR, Wu M, Huang CY, Harris WP, Sim HG, Lucas JM, *et al.* Chemotherapy-induced monoamine oxidase expression in prostate carcinoma functions as a cytoprotective resistance enzyme and associates with clinical outcomes. PLoS One. 2014;9(9):e104271.
9. Shigeta K, Kosaka T, Yazawa S, Yasumizu Y, Mizuno R, Nagata H, *et al.* Predictive factors for severe and febrile neutropenia during docetaxel chemotherapy for castration-resistant prostate cancer. Int J Clin Oncol. 2014. doi:10.1007/s10147-014-0746-7.
10. LaRocque J, Bharali DJ, Mousa SA. Cancer detection and treatment: the role of nanomedicines. Mol Biotechnol. 2009;42(3):358–66.
11. Raghow S, Hooshdaran MZ, Katiyar S, Steiner MS. Toremifene prevents prostate cancer in the transgenic adenocarcinoma of mouse prostate model. Cancer Res. 2002;62(5):1370–6.
12. Mousa SA, Bharali DJ. Nanotechnology-based detection and targeted therapy in cancer: nano-bio paradigms and applications. Cancers. 2011;3(3):2888–903.
13. Holzmann C, Kilch T, Kappel S, Armbruster A, Jung V, Stockle M, *et al.* ICRAC controls the rapid androgen response in human primary prostate epithelial cells and is altered in prostate cancer. Oncotarget. 2013;4(11):2096–107.
14. Sokoloff RL, Norton KC, Gasior CL, Marker KM, Grauer LS. A dual-monoclonal sandwich assay for prostate-specific membrane antigen: levels in tissues, seminal fluid and urine. Prostate. 2000;43(2):150–7.
15. Ristau BT, O'Keefe DS, Bacich DJ. The prostate-specific membrane antigen: lessons and current clinical implications from 20 years of research. Urol Oncol. 2013;32(3):272–9.
16. Troyer JK, Beckett ML, Wright Jr GL. Detection and characterization of the prostate-specific membrane antigen (PSMA) in tissue extracts and body fluids. Int J Cancer. 1995;62(5):552–8.
17. Cao KY, Xu L, Zhang DM, Zhang XM, Zhang T, He X, *et al.* New alternatively spliced variant of prostate-specific membrane antigen PSM-E suppresses the proliferation, migration and invasiveness of prostate cancer cells. Int J Oncol. 2012;40(6):1977–85.
18. Su SL, Huang IP, Fair WR, Powell CT, Heston WD. Alternatively spliced variants of prostate-specific membrane antigen RNA: ratio of expression as a potential measurement of progression. Cancer Res. 1995;55(7):1441–3.
19. Akhtar NH, Pail O, Saran A, Tyrell L, Tagawa ST. Prostate-specific membrane antigen-based therapeutics. Adv Urol. 2012;2012:Article ID 973820.
20. Chang SS. Overview of prostate-specific membrane antigen. Rev Urol. 2004;6 Suppl 10:S13–8.
21. Bonkhoff H, Berges R. The evolving role of oestrogens and their receptors in the development and progression of prostate cancer. Eur Urol. 2009;55(3):533–42.
22. Price D, Stein B, Sieber P, Tutrone R, Bailen J, Goluboff E, *et al.* Toremifene for the prevention of prostate cancer in men with high grade prostatic intraepithelial neoplasia: results of a double-blind, placebo controlled, phase IIB clinical trial. J Urol. 2006;176(3):965–70. discussion 970–961.
23. Matthews J, Gustafsson JA. Estrogen signaling: a subtle balance between ER alpha and ER beta. Mol Interv. 2003;3(5):281–92.

24. Bharali DJ, Yalcin M, Davis PJ, Mousa SA. Tetraiodothyroacetic acid-conjugated PLGA nanoparticles: a nanomedicine approach to treat drug-resistant breast cancer. Nanomedicine. 2013;8(12): 1943–54.
25. Cho HS, Dong Z, Pauletti GM, Zhang J, Xu H, Gu H, *et al.* Fluorescent, superparamagnetic nanospheres for drug storage, targeting, and imaging: a multifunctional nanocarrier system for cancer diagnosis and treatment. ACS Nano. 2010;4(9):5398–404.
26. Graf N, Bielenberg DR, Kolishetti N, Muus C, Banyard J, Farokhzad OC, *et al.* alpha(V)beta(3) integrin-targeted PLGA-PEG nanoparticles for enhanced anti-tumor efficacy of a Pt(IV) prodrug. ACS Nano. 2012;6(5):4530–9.
27. Bansal G, Maddhesia PK, Bansal Y. MS2/TOF and LC-MS/TOF studies on toremifene to characterize its forced degradation products. Analyst. 2011;136(24):5218–28.
28. Mazzarino M, Fiacco I, de la Torre X, Botre F. A mass spectrometric approach for the study of the metabolism of clomiphene, tamoxifen and toremifene by liquid chromatography time-of-flight spectroscopy. Eur J Mass Spectrom. 2008;14(3):171–80.
29. Sumantran VN. Cellular chemosensitivity assays: an overview. Methods Mol Biol. 2011;731:219–36.
30. Gao X, Yang L, Petros JA, Marshall FF, Simons JW, Nie S. In vivo molecular and cellular imaging with quantum dots. Curr Opin Biotechnol. 2005;16(1):63–72.
31. Kim IY, Kim BC, Seong DH, Lee DK, Seo JM, Hong YJ, *et al.* Raloxifene, a mixed estrogen agonist/antagonist, induces apoptosis in androgen-independent human prostate cancer cell lines. Cancer Res. 2002;62(18):5365–9.
32. Lopes AD, Davis WL, Rosenstraus MJ, Uveges AJ, Gilman SC. Immunohistochemical and pharmacokinetic characterization of the site-specific immunoconjugate CYT-356 derived from antiprostate monoclonal antibody 7E11-C5. Cancer Res. 1990;50(19):6423–9.